

Influence of Behavioral Models on Multiuser Channel Capacity

Erik Agrell, *Senior Member, IEEE*, and Magnus Karlsson, *Fellow, OSA; Senior Member, IEEE*

Abstract—In order to characterize the channel capacity of a wavelength channel in a wavelength-division multiplexed (WDM) system, statistical models are needed for the transmitted signals on the other wavelengths. For example, one could assume that the transmitters for all wavelengths are configured independently of each other, that they use the same signal power, or that they use the same modulation format. In this paper, it is shown that these so-called behavioral models have a profound impact on the single-wavelength achievable information rate. This is demonstrated by establishing, for the first time, upper and lower bounds on the maximum achievable rate under various behavioral models, for a rudimentary WDM channel model.

Index Terms—Achievable information rate, behavioral models, channel capacity, multiuser communications, mutual information, network information theory, nonlinear interference, wavelength-division multiplexing.

I. INTRODUCTION

One of Shannon’s most significant contributions was the definition of the *channel capacity* as the highest achievable throughput (in bit/symbol or bit/s/Hz) of a given communication channel, at an arbitrarily low error probability [1]. He furthermore showed that a capacity-achieving transmission scheme can operate by transmitting discrete-time symbols generated from a suitably chosen *input distribution*, if certain conditions are imposed on the allowed sequences of symbols.

In a more practical setting, the symbols correspond to pulses, the input distribution to a modulation format, and the allowed sequences of symbols to an error-correcting code. The maximum throughput that can be achieved with the best possible error-correcting code is, for a given channel and a given input distribution, given by the *mutual information* [2, Ch. 2, 7]. This quantity can be expressed as a (possibly complicated but still explicit) integral over the joint distribution of the transmitted and received symbols. Thus, it is a function of the channel and the input distribution. To obtain the channel capacity, which is a function of the channel alone, the mutual information should therefore be maximized over all possible input distributions (or modulation formats). Neither this maximization nor the mutual information integral admit analytical solutions in general, and the exact channel capacity is therefore known only for a few specific channels, of which

the additive white Gaussian noise (AWGN) channel is the most well known. This implies that for most practical channels, the capacity is only known in terms of upper and lower bounds.

For the coherent fiber-optic channel, the AWGN channel model is a good starting point, due to the amplified spontaneous emission (ASE) noise in optical amplifiers, but the nonlinearities of the optical fiber will make this channel model inaccurate for sufficiently high signal powers. Assuming the added ASE noise variance P_{ase} to be fixed and known, the question is, how will the channel capacity $C(P)$ behave as a function of the signal power P ? There is a common and reasonable belief [3]–[5] that the nonlinearity will somehow limit the available capacity for fiber links, but the question is to what extent.

For the single-wavelength channel, the capacity was pioneered in [3], where it was shown to reach a maximum and then decay as the signal power increases, and more recently referred to as the “nonlinear Shannon limit” [6], [7]. However, more or less all such plots formally represent *lower bounds* on the channel capacity, as pointed out, e.g., in [4], [8]–[10], since they are obtained from analysis over a finite set over all possible input distributions or using suboptimal (mismatched) receivers. It is possible to show that the channel capacity will not decay at high signal powers, provided that a sufficiently exhaustive search over input distributions is carried out at each signal power level [11], [12]. Moreover, it can be shown that the use of a *finite-memory channel model* will also raise the lower capacity bounds at high signal powers to nonzero values [13].

In this paper, which is an extension of [14], we will deal with the capacity of *multichannel systems*, e.g., wavelength-division multiplexed (WDM) optical links, for which the situation is more subtle. The current paradigm in optical multiuser communications [4]–[7], [9], [15]–[26] is to analyze the capacity of a single user in the system, say user 1, assuming that the other users are outside our control. We will therefore call user 1 the *primary user* and the other users, whose transmissions cause interference to user 1, *interferers*. More formally, the quantity of interest is the achievable information rate $C_1 = \sup I(X_1; Y_1)$, where $I(X_1; Y_1)$ denotes the mutual information between the input X_1 and output Y_1 of subchannel 1, and the maximization is over all possible input distributions (modulation formats) f_{X_1} . These quantities will be mathematically defined in Sec. IV, where it is also remarked that C_1 is in general not a channel capacity in the information-theoretic sense. It is instructive to contrast with wireless multiuser systems, where the transmitters are typically designed jointly (but possibly operated separately),

This work was supported in part by the Swedish Research Council (VR) under grants 2012-5280 and 2013-5271. The material in this paper was presented in part at the Optical Fiber Communication Conference (OFC), Anaheim, CA, Mar. 2013.

E. Agrell is with the Dept. of Signals and Systems, Chalmers Univ. of Technology, SE-41296 Göteborg, Sweden, email agrell@chalmers.se. M. Karlsson is with the Dept. of Microtechnology and Nanoscience, Chalmers Univ. of Technology, SE-41296 Göteborg, Sweden.

and the relevant capacity measure is a multidimensional object, the *capacity region*, which describes the set of achievable throughputs for all users simultaneously [27], [2, Ch. 15], [28, Ch. 6].

Two kinds of models are needed to fully describe a multiuser system as a single-user channel model $X_1 \rightarrow Y_1$, as illustrated in Fig. 1: the first is a discrete-time multiuser channel model, which gives the statistics of the channel outputs Y_1, \dots, Y_M as functions of the inputs X_1, \dots, X_M , and the second is a *behavioral model*, which relates the interferers' distributions f_{X_2}, \dots, f_{X_M} to the primary user input distribution f_{X_1} . Obviously, f_{X_1} needs to be optimized for the considered multiuser channel model in order to attain the channel capacity, but how shall the interferers, which cause interference to the primary user, behave during this optimization process? Will they be passive, or are they allowed to adapt their signaling power and/or modulation format to the power and/or modulation format of the primary user? These questions are usually not explicitly addressed in the majority of papers on optical multiuser capacity. The notable exception is the work by Taghavi *et al.* [27], where both the capacity region and some bounds thereon were defined for a WDM system model, based on a Volterra approach. Their main conclusion (based on simulations of a simplified, nonlinear channel model) was that $C_1(P)$ is unbounded if the receiver could use multiuser detection to cancel nonlinear interference, and saturated (monotonically) to a constant value in the special case of increasing all user powers P simultaneously.

In this paper, we discuss and classify the different behavioral models used in the literature, and give an illustrative example of multiuser capacity for a simple nonlinear optical channel model, together with some general conclusions on how the selected behavioral model for the interferers influences $C_1(P)$. Although the idealized channel model is not fully realistic, it serves the purpose of exemplifying, for the first time, the profound impact of behavioral models on the nonlinear channel capacity. The paper is organized as follows. In Sec. II, the multiuser nonlinear channel model is described and its parameters are defined. The behavioral models are defined in Sec. III, where we also attempt to classify the behavioral models considered in earlier optical channel capacity studies. After mathematically defining the channel capacity and related quantities in Sec. IV, upper and lower bounds are derived in Sec. V and VI, resp. The obtained bounds are plotted and discussed in Sec. VII. The paper concludes in Sec. VIII with a discussion about the validity of the results and their potential extensions to more realistic optical channel models.

We use uppercase notation X for random variables and lowercase x for deterministic variables. Probability density functions are denoted as $f_X(x)$ and conditional probability density functions as $f_{Y|X}(y|x)$, where the subscripts will sometimes be omitted if they are clear from the context.

II. SYSTEM MODEL

In order to exemplify the information-theoretic nature of various behavioral models in optical communications, we need a simple, yet nontrivial, channel model for a WDM link,

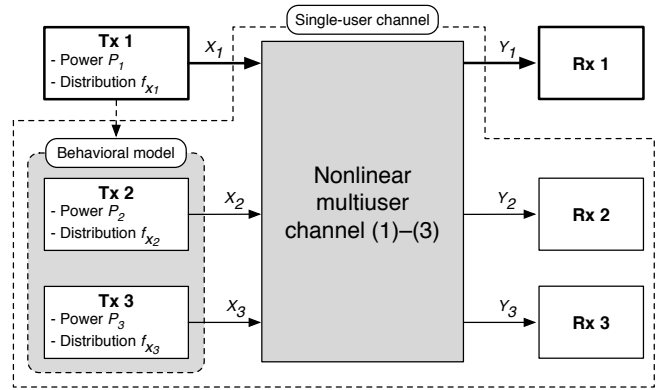


Fig. 1. A single-user channel model can be seen as a combination of a multiuser channel model and a behavioral model for all users but one. Transmitter and receiver are marked Tx and Rx, respectively.

which enables analytical and numerical calculations of upper and lower bounds on the achievable rates. Linear modulation is used in the transmitter, and the receiver applies coherent matched filtering and sampling. We select a simplified model with three equispaced WDM channels enumerated by $i = 1, 2, 3$. For simplicity, we assume that four-wave mixing dominates over self- and cross-phase modulation. This scenario arises, e.g., when the generalized phase-matching condition is fulfilled [29]. The dispersion and the nonlinearity are both assumed weak, which means that the nonlinear phase shift $\phi_{NL} \ll 1$. Under these assumptions, the coupled nonlinear differential equations can be linearized in propagation distance by a perturbative analysis. A detailed discussion and the full set of coupled equations for this situation can be found in [29]. We find that the complex discrete-time output signals Y_i are given by a nonlinear channel model according to

$$Y_1 = X_1 + \epsilon X_2^2 X_3^* + N_1, \quad (1)$$

$$Y_2 = X_2 + 2\epsilon X_1 X_2^* X_3 + N_2, \quad (2)$$

$$Y_3 = X_3 + \epsilon X_1^* X_2^2 + N_3, \quad (3)$$

where X_i are independent, complex channel inputs and N_i are independent, complex, circularly symmetric, white Gaussian noise signals, each with zero mean and equal variance. The indices in (1)–(3) are the same as in [27, Eq. (8)], [30, Eq. (6)], confining the WDM system to 3 wavelengths and ignoring self- and cross-phase modulation terms. Similar models were derived in the context of noncoherent WDM systems with on-off keying modulation [31], [32]. As in [27] and other works, our intention is *not* to present an accurate channel model, but rather the opposite: We wish to use the simplest possible nonlinear WDM model that will allow us to qualitatively compare different behavioral models.

In this work, we consider the *single-wavelength detection* scenario, as it was defined in [27]. This means that each receiver i receives its own signal Y_i , with no information about the other received signals Y_j for $j \neq i$. Furthermore, receiver i knows the distributions f_{X_j} of the other users $j \neq i$, but not their codebooks. Hence, multiuser detection [27], [33], [34] is possible, but not simultaneous decoding [28, Ch. 6].

The channel model (1)–(3) is characterized by two parameters, ϵ and $P_{\text{ase}} = \mathbb{E}[|N_i|^2]$. In an n -span amplified link, the single-polarization noise variance (power) equals $P_{\text{ase}} = nn_{\text{sp}}(G - 1)h\nu B$, where n_{sp} is the spontaneous emission factor, $h\nu$ the photon energy, G the gain of each amplifier, which also equals the span loss, and B the signal bandwidth. The constant in (1)–(3) is $\epsilon = n\gamma L_{\text{eff}}$, where γ is the fiber nonlinear coefficient and L_{eff} the effective nonlinear amplifier span length, related to the physical amplifier separation L via $L_{\text{eff}} = (1 - \exp(-\alpha L))/\alpha$ with α being the fiber attenuation coefficient. One may improve the model by multiplying ϵ with a complex factor depending on the phase mismatch, attenuation factor, and span length, but we neglect this for simplicity.

For the numerical examples in Sec. VII, the following parameters will be used. We consider a link with $n = 16$ amplifier spans. The gain of each is $G = 30$ dB and the spontaneous emission factor is $n_{\text{sp}} = 2$. The signal bandwidth is $B = 40$ GHz, and with $h\nu = 0.128$ aJ, $\gamma = 1.6$ W⁻¹ km⁻¹, and $L_{\text{eff}} = 24$ km, we get $P_{\text{ase}} = 0.16$ mW and $\epsilon = 610$ W⁻¹. The condition $\phi_{NL} = \epsilon P \ll 1$, where P is the signal power, translates to $P \ll 1.6$ mW, or a signal-to-noise ratio of $P/P_{\text{ase}} < 10$ dB. We will apply this model, which was derived under a weak nonlinearity assumption, also in the strongly nonlinear regime, which although inaccurate is the conventional approach in the literature.

III. BEHAVIORAL MODELS IN MULTIUSER COMMUNICATIONS

Whenever a multiuser system is characterized by means of a single-user channel capacity, the results are connected to a certain behavioral model, as discussed above. The behavioral models relate the input distributions of the interferers to the primary input distribution. We study three fundamentally different classes of behavioral models:

- (a) *Fixed interferer distributions.* The interferer distributions f_{X_2}, \dots, f_{X_M} remain the same regardless of f_{X_1} . The dashed arrow from Tx 1 in Fig. 1 does not exist in this case. From the viewpoint of information theory, this is a single-user channel.
- (b) *Adaptive interferer power.* All users transmit with the same power $P_1 = P_2 = P_3$, but not necessarily the same distributions. The interferer distributions f_{X_2}, \dots, f_{X_M} are fixed apart from a scale factor, which depends on P_1 .
- (c) *Adaptive interferer distribution.* All users transmit with the same distribution and the same power, $f_{X_1} = f_{X_2} = f_{X_3}$.

The channel models used for WDM capacity analyses in the literature fall in categories (b) and (c). Model (b) was used by Wegener *et al.* [20], where on–off keying modulation was assumed for the interferers [20, Eq. (15)], and a Gaussian pdf assumed for the primary user, although all users had the same power. Behavioral model (b) was also considered in [26, Fig. 2(b)], where the influence of interferer distributions on the achievable rate of the primary user was studied. It was concluded that Gaussian interferers caused worse interference than quadrature phase-shift keying (QPSK) and ring-shaped

modulation, when the primary user applies Gaussian modulation at the same power level as the interferers. Model (c) was used in [5], [7], [9], [22], [25]–[27], where it was explicitly stated that every channel had the same modulation and power. Multilevel ring-shaped modulation was used in [5], [7], [9], [22], [25], four different modulation formats were used in [26, Fig. 2(a)], and Gaussian modulation for all channels was used in [27]. Quite a few studies have used models of the nonlinear interference that does not depend on the choice of modulation format, but only on the power spectral density of the interferers. Then the modulation of the interferers has not been specified, and the chosen behavioral model can be either (b) or (c). This applies to [4], [6], [15]–[19], [21], [23], [24].

As will be demonstrated in the following, the achievable rates may vary significantly between behavioral models.

IV. INFORMATION THEORY

The mutual information between two random variables X and Y with joint distribution $f_{X,Y}$ and marginal distributions $f_X(x) = \int f_{X,Y}(x,y)dy$ and $f_Y(y) = \int f_{X,Y}(x,y)dx$ is defined as [2, Eq. (2.35)]

$$I(X; Y) = \iint f_{X,Y}(x,y) \log_2 \frac{f_{X,Y}(x,y)}{f_X(x)f_Y(y)} dx dy, \quad (4)$$

where the integral is over the domain of X and Y . If one or both of X and Y are discrete, their distributions are replaced with probability mass functions and the corresponding integrals are replaced with sums. Similarly, the *conditional mutual information* between X and Y given another random variable Z is defined as [2, Eq. (2.61)]

$$I(X; Y|Z) = \iiint f_{X,Y|Z}(x,y|z) \log_2 \frac{f_{X,Y|Z}(x,y|z)}{f_{X|Z}(x|z)f_{Y|Z}(y|z)} dx dy dz.$$

If X and Y are the input and output, resp., of a communication channel, then the joint distribution can be separated into the product $f_{X,Y}(x,y) = f_X(x)f_{Y|X}(y|x)$, where f_X denotes the *input distribution* and $f_{Y|X}$ denotes the *channel*. Thus, the mutual information depends on both the input distribution and the channel. More precisely, the mutual information gives the highest achievable rate, in bit/symbol, of a given channel and a given input distribution, if strong coding is allowed over long blocks of symbols. As discussed in the Introduction, the channel capacity is

$$C = \sup_{f_X} I(X; Y), \quad (5)$$

which is a function of the channel only, not of the input distribution. From a practical viewpoint, the optimization over input distributions in (5) can be regarded as an optimization over modulation formats.

In the multiuser scenario considered in this paper, we are interested in the channel capacity of one subchannel. Inspired by (5), one can define

$$C_i(P_i) = \sup_{f_{X_i}: \mathbb{E}[|X_i|^2]=P_i} I(X_i; Y_i), \quad (6)$$

where $P_i = \mathbb{E}[|X_i|^2] = \int |x|^2 f_{X_i}(x) dx$ is the signal power of subchannel i . This quantity is an achievable rate of subchannel i and has been studied in numerous publications in optical communications. It is often called the channel capacity, although, strictly speaking, the single-user channels in Fig. 1 have no channel capacity in an information-theoretic sense, since Shannon's channel coding theorem, according to which (5) gives the maximum achievable rate of the channel described by $f_{Y|X}$, assumes the channel law $f_{Y|X}$ to remain the same throughout the maximization. This is not the case in (6), where $I(X_i; Y_i)$ relies on a channel law $f_{Y_i|X_i}$ that changes with f_{X_i} and/or P_i , according to the behavioral models that control the input distributions f_{X_j} for $j \neq i$.

In this paper, we wish to evaluate $C_1(P_1)$ for the behavioral models in Sec. III.¹ As usual in nonlinear information theory, it seems infeasible to find an exact expression, but we can follow the standard approach and sandwich the achievable rates between upper and lower bounds. No approximations are involved in the derivations of these bounds.

V. UPPER BOUNDS

Our upper bounds on C_1 depend on the following fundamental lemma.

Lemma 1: If X and Z are independent, then

$$I(X; Y) \leq I(X; Y|Z)$$

Proof: From [2, Eq. (2.119–120)],

$$I(X; Y|Z) = I(X; Y) + I(X; Z|Y) - I(X; Z) \quad (7)$$

$$= I(X; Y) + I(X; Z|Y) \quad (8)$$

$$\geq I(X; Y),$$

where (7) follows from the independence of X and Z and (8) from the nonnegativity of conditional mutual information [2, Eq. (2.92)]. \square

If X and Z are not independent, the Lemma does not hold. A notable example is when $X \rightarrow Y \rightarrow Z$ forms a Markov chain, in which case $I(X; Y|Z) \leq I(X; Y)$ follows by the data-processing inequality [2, Eq. (2.122)].

For the specific channel model (1), the lemma can be used to derive two upper bounds.

Theorem 2: For any distributions of X_2 and X_3 , C_1 is upperbounded as

$$C_1(P_1) \leq \log_2 \left(1 + \frac{P_1}{P_{\text{ase}}} \right)$$

Proof: From (6) and Lemma 1,

$$C_1(P_1) \leq \sup_{f_{X_1; \mathbb{E}[|X_1|^2]=P_1}} I(X_1; Y_1|X_2, X_3). \quad (9)$$

Given $X_2 = x_2$ and $X_3 = x_3$, (1) is an AWGN channel with a constant offset $\epsilon x_2^2 x_3^*$. If this offset is known, it can be subtracted at the receiver, resulting in a regular zero-mean AWGN channel with noise variance $\mathbb{E}[|N_1|^2] = P_{\text{ase}}$.

¹A similar analysis can be carried out for subchannels 2 and 3. By symmetry, $C_3(P_3)$ is equivalent to $C_1(P_1)$, whereas $C_2(P_2)$ is different. Some of the bounds in Sec. V and VI extend straightforwardly to C_2 as well (e.g., Theorems 4 and 5), whereas other bounding techniques, tailored to (2), would be needed for a full characterization of $C_2(P_2)$.

Hence, the right-hand side of (9) equals the AWGN channel capacity $\log_2(1 + P_1/P_{\text{ase}})$, independently of x_2 and x_3 , which completes the proof. \square

Alternatively, the theorem can be derived from (1) via the data-processing inequality [2, Th. 2.8.1].

Theorem 2 holds for any distributions of X_2 and X_3 , and therefore for any behavioral models. For certain behavioral models, the bound can be tightened using the next theorem.

Theorem 3: If X_2 and X_3 are zero-mean, circularly symmetric Gaussian (ZCG), then

$$C_1(P_1) \leq \frac{1}{P_2} \int_0^\infty e^{-u/P_2} \log_2 \left(1 + \frac{P_1}{P_{\text{ase}} + \epsilon^2 P_3 u^2} \right) du$$

Proof: Invoking Lemma 1, this time conditioning on X_2 only, yields

$$\begin{aligned} C_1(P_1) &\leq \sup I(X_1; Y_1|X_2) \\ &= \sup \int_{\mathbb{C}} f(x_2) I(X_1; Y_1|X_2 = x_2) dx_2 \\ &\leq \int_{\mathbb{C}} f(x_2) \sup I(X_1; Y_1|X_2 = x_2) dx_2, \end{aligned} \quad (10)$$

where the suprema are over all f_{X_1} such that $\mathbb{E}[|X_1|^2] = P_1$. If X_3 is Gaussian, then (1) conditioned on $X_2 = x_2$ is a zero-mean AWGN channel, because its two noise contributions $\epsilon x_2^2 X_3^*$ and N_1 are both Gaussian. The power of $\epsilon x_2^2 X_3^*$ is $\epsilon^2 |x_2|^4 P_3$, while the power of N_1 is P_{ase} as before. Hence, the supremum in (10) equals the capacity of an AWGN channel with power $P_{\text{ase}} + \epsilon^2 |x_2|^4 P_3$,

$$C_1(P_1) \leq \int_{\mathbb{C}} f(x_2) \log_2 \left(1 + \frac{P_1}{P_{\text{ase}} + \epsilon^2 |x_2|^4 P_3} \right) dx_2. \quad (11)$$

This bound can be simplified by using the circular symmetry of

$$f(x_2) = \frac{1}{\pi P_2} e^{-|x_2|^2/P_2}.$$

Let $U = |X_2|^2$. Then U is exponentially distributed,

$$f(u) = \frac{1}{P_2} e^{-u/P_2}, \quad u \geq 0. \quad (12)$$

The theorem now follows by changing the integration variable in (11) from x_2 to $u = |x|^2$. \square

VI. LOWER BOUNDS

Since the channel capacity is the supremum of mutual information, a lower bound on capacity can be obtained from the mutual information for any given input distribution. Analogously, from (6),

$$C_1(P_1) \geq I(X_1; Y_1) \quad (13)$$

for any input distribution f_{X_1} with power P_1 . In this section, we will obtain lower bounds on $C_1(P_1)$ via (13).

If all input distributions are discrete, it is feasible to calculate the right-hand side of (13) by numerical integration, using either of the following two theorems.

Theorem 4: If X_1 , X_2 , and X_3 are all discrete, uniformly distributed over complex constellations \mathcal{X}_1 , \mathcal{X}_2 , and \mathcal{X}_3 , resp., then

$$I(X_1; Y_1) = \mathbb{E} \left[\log_2 \frac{f(y_1|x_1)}{f(y_1)} \right], \quad (14)$$

where

$$f(y_1|x_1) = \frac{1}{\pi P_{\text{ase}} |\mathcal{X}_2| |\mathcal{X}_3|} \sum_{x_2 \in \mathcal{X}_2} \sum_{x_3 \in \mathcal{X}_3} \exp \left(-\frac{|y_1 - x_1 - \epsilon x_2^2 x_3^*|^2}{P_{\text{ase}}} \right), \quad (15)$$

$$f(y_1) = \frac{1}{|\mathcal{X}_1|} \sum_{x_1 \in \mathcal{X}_1} f(y_1|x_1). \quad (16)$$

Proof: From (1),

$$f(y_1|x_1, x_2, x_3) = \frac{1}{\pi P_{\text{ase}}} \exp \left(-\frac{|y_1 - x_1 - \epsilon x_2^2 x_3^*|^2}{P_{\text{ase}}} \right). \quad (17)$$

Marginalizing $f(y_1|x_1, x_2, x_3)$ yields $f(y_1|x_1)$ and $f(y_1)$. Finally, (14) follows by rewriting (4). \square

Theorem 5: If X_1 is ZCG and X_2 and X_3 are discrete, uniformly distributed over complex constellations \mathcal{X}_2 and \mathcal{X}_3 , resp., then

$$I(X_1; Y_1) = \mathbb{E} \left[\log_2 \frac{f(y_1|x_1)}{f(y_1)} \right], \quad (18)$$

where

$$f(y_1|x_1) = \frac{1}{\pi P_{\text{ase}} |\mathcal{X}_2| |\mathcal{X}_3|} \sum_{x_2 \in \mathcal{X}_2} \sum_{x_3 \in \mathcal{X}_3} \exp \left(-\frac{|y_1 - x_1 - \epsilon x_2^2 x_3^*|^2}{P_{\text{ase}}} \right), \quad (19)$$

$$f(y_1) = \frac{1}{\pi (P_1 + P_{\text{ase}}) |\mathcal{X}_2| |\mathcal{X}_3|} \sum_{x_2 \in \mathcal{X}_2} \sum_{x_3 \in \mathcal{X}_3} \exp \left(-\frac{|y_1 - \epsilon x_2^2 x_3^*|^2}{P_1 + P_{\text{ase}}} \right). \quad (20)$$

Proof: In (1), $X_1 + N_1$ is ZCG with variance $P_1 + P_{\text{ase}}$, which yields

$$f(y_1|x_2, x_3) = \frac{1}{\pi (P_1 + P_{\text{ase}})} \exp \left(-\frac{|y_1 - \epsilon x_2^2 x_3^*|^2}{P_1 + P_{\text{ase}}} \right).$$

Marginalizing this distribution with respect to X_2 and X_3 yields $f(y_1)$ in (20). Equation (19) is proved as in the proof of Theorem 4, which completes the proof of (18). \square

In Sec. VII, the expectations in (14) and (18) will be evaluated by Monte-Carlo integration to obtain lower bounds on C_1 via (13). Theorem 4 applies to all three behavioral models, as long as the interferer distributions X_2 and X_3 are discrete, whereas Theorem 5 applies to some cases of models (a) and (b).

Theoretically, Theorems 4 and 5 can be modified to hold also when at least one of the input distributions is continuous. In this case, the corresponding sums in the expressions for $f(y_1|x_1)$ and $f(y_1)$ will be replaced by integrals. However, these integrals cannot in general be evaluated analytically. This causes numerical problems in (14) and (18), where the

Monte-Carlo estimate of the expectation may become grossly inaccurate if $f(y_1|x_1)$ is not exact. Applying Monte-Carlo integration inside another Monte-Carlo integral should be avoided if at all possible. Therefore, we wish to find other lower bounds on the mutual information. To this end, the following lemma, due to Emre Telatar, is useful. It was stated and proved in [4], [20], and it can also be obtained as a special case of the *auxiliary-channel lower bound* [35, Sec. VI]².

Lemma 6: Let X_G and Y_G be complex, dependent, jointly Gaussian random variables. Let Y be any complex random variable (possibly non-Gaussian) such that

$$\begin{aligned} \mathbb{E}[|Y|^2] &= \mathbb{E}[|Y_G|^2], \\ \mathbb{E}[Y^* X_G] &= \mathbb{E}[Y_G^* X_G]. \end{aligned}$$

Then

$$I(X_G; Y) \geq I(X_G; Y_G).$$

The next lemma gives the mutual information of two complex, jointly Gaussian variables. It is proved by straightforward evaluation of the integral in (4); see, e.g., [36, Eq. (9-8)].

Lemma 7: If X_G and Y_G are complex, jointly Gaussian variables with zero mean, variances $\mathbb{E}[|X_G|^2] = \sigma_X^2$ and $\mathbb{E}[|Y_G|^2] = \sigma_Y^2$, resp., and covariance $\mathbb{E}[X_G Y_G^*] = s_{XY}$, then their mutual information is

$$I(X_G; Y_G) = \log_2 \frac{\sigma_X^2 \sigma_Y^2}{\sigma_X^2 \sigma_Y^2 - |s_{XY}|^2}.$$

The preceding two lemmas make it possible to prove the following lower bound.

Theorem 8: For any zero-mean interferer distributions f_{X_2} and f_{X_3} ,

$$C_1(P_1) \geq \log_2 \left(1 + \frac{P_1}{\epsilon^2 P_3 \mathbb{E}[|X_2|^4] + P_{\text{ase}}} \right). \quad (21)$$

Proof: Combining (13) with Lemmas 6 and 7 yields

$$C_1(P_1) \geq \log_2 \frac{P_1 \sigma_Y^2}{P_1 \sigma_Y^2 - |s_{XY}|^2}, \quad (22)$$

where

$$\begin{aligned} \sigma_Y^2 &= \mathbb{E}[|Y_1|^2], \\ s_{XY} &= \mathbb{E}[X_1 Y_1^*], \end{aligned}$$

and Y_1 is given by (1) for a ZCG input distribution X_1 . Using the independence of X_1 , X_2 , and X_3 ,

$$\begin{aligned} \sigma_Y^2 &= \mathbb{E}[|X_1 + \epsilon X_2^2 X_3^* + N_1|^2] \\ &= \mathbb{E}[|X_1|^2] + \epsilon^2 \mathbb{E}[|X_2|^4] \mathbb{E}[|X_3|^2] + \mathbb{E}[|N_1|^2] \\ &= P_1 + \epsilon^2 P_3 \mathbb{E}[|X_2|^4] + P_{\text{ase}}, \end{aligned} \quad (23)$$

$$\begin{aligned} s_{XY} &= \mathbb{E}[X_1 (X_1 + \epsilon X_2^2 X_3^* + N_1)^*] \\ &= \mathbb{E}[|X_1|^2] \\ &= P_1. \end{aligned} \quad (24)$$

The theorem now follows by substituting (23)–(24) into (22) and simplifying. \square

²To see this, substitute $X = X_G$, $p(x) = p_G(x)$, $q(y|x) = p_G(x, y)/p_G(x)$, and $q_p(y) = p_G(y)$ in [35, Eq. (34)].

The right-hand side of (21) depends on the statistics of X_2 . For example, if X_2 is discrete, uniformly distributed over a constellation \mathcal{X}_2 , then

$$\mathbb{E}[|X_2|^4] = \frac{1}{|\mathcal{X}_2|} \sum_{x \in \mathcal{X}_2} |x|^4. \quad (25)$$

In the special case of a phase-shift keying (PSK) constellation with power P_2 , (25) simplifies into $\mathbb{E}[|X_2|^4] = P_2^2$.

On the other hand, if X_2 is ZCG, then $\mathbb{E}[|X_2|^4]$ can be calculated by setting $X_2 = X_r + jX_i$, where $j = \sqrt{-1}$ and X_r and X_i are real, independent, Gaussian variables with zero mean and variance $\sigma^2 = P_2/2$. Then

$$\begin{aligned} \mathbb{E}[|X_2|^4] &= \mathbb{E}[|X_r + jX_i|^4] \\ &= \mathbb{E}[X_r^4] + \mathbb{E}[X_i^4] + 2\mathbb{E}[X_r^2]\mathbb{E}[X_i^2] \\ &= 3\sigma^4 + 3\sigma^4 + 2\sigma^2\sigma^2 \end{aligned} \quad (26)$$

$$= 2P_2^2, \quad (27)$$

where (26) follows from a standard result in mathematical statistics [37, Eq. (5-46)].

Theorem 8 will be used in the next section to lower-bound C_1 in certain cases when the interference is governed by behavioral models (a) or (b).

VII. RESULTS

In this section, the bounds of Sec. VI and V are numerically evaluated for the multiuser channel (1)–(3), using the parameters ϵ and P_{ase} as specified in Sec. II. Fig. 2 (a)–(c) illustrate via upper and lower bounds the single-user achievable rates $C_1(P_1) = \sup I(X_1; Y_1)$, where the maximization is over all distributions f_{X_1} with power P_1 , combined with the three behavioral models in Sec. III. For models (a) and (b), the interferer distributions f_{X_2} and f_{X_3} are either uniform over a QPSK constellation or Gaussian, which in total gives five scenarios. We will discuss the three models separately below.

A. Behavioral model (a)—fixed interferer distributions

With behavioral model (a), the interferer distributions f_{X_2} and f_{X_3} are fixed and do not change with f_{X_1} . The interference power is also fixed at a level of $P_2/P_{\text{ase}} = P_3/P_{\text{ase}} = 5$ dB. The applied bounds are different depending on the nature of the interferers: If X_2 and X_3 follow QPSK distributions, then we obtain an upper bound from Theorem 2 and a lower bound from Theorem 5 or 8, where Monte Carlo integration was used to estimate the expectation in (18). The two lower bounds turn out to be numerically indistinguishable; in Fig. 2 (a), Theorem 5 is plotted. On the other hand, if X_2 and X_3 follow Gaussian distributions, our upper bound is given by Theorem 3 and the lower bound by Theorem 8 and (27).

The upper and lower bounds follow each other and together prove that the achievable rate increases to infinity if the signal power can be increased arbitrarily. This result is not surprising, since X_1 dominates over the two other terms in (1) at sufficiently high power P_1 . The channel is in fact a single-user channel, described by a fixed distribution $f_{Y_1|X_1}$, and the channel capacity is nondecreasing for all such channels, linear or nonlinear [12]. The capacity is larger in the case of

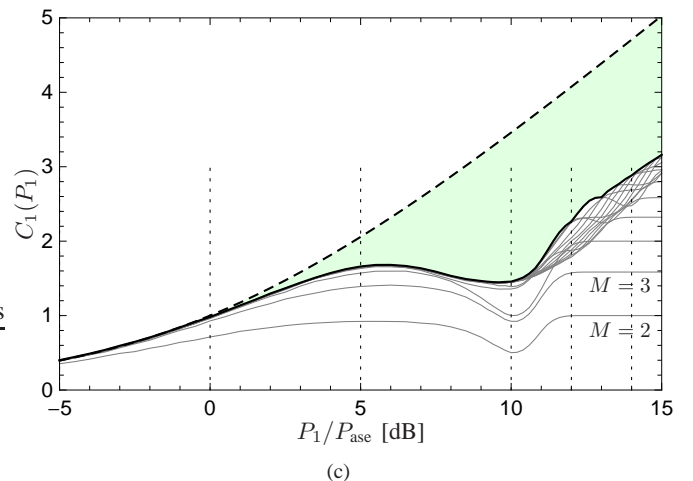
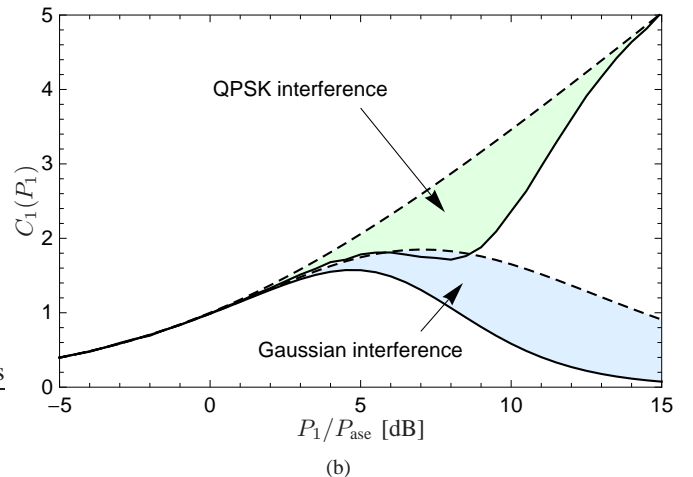
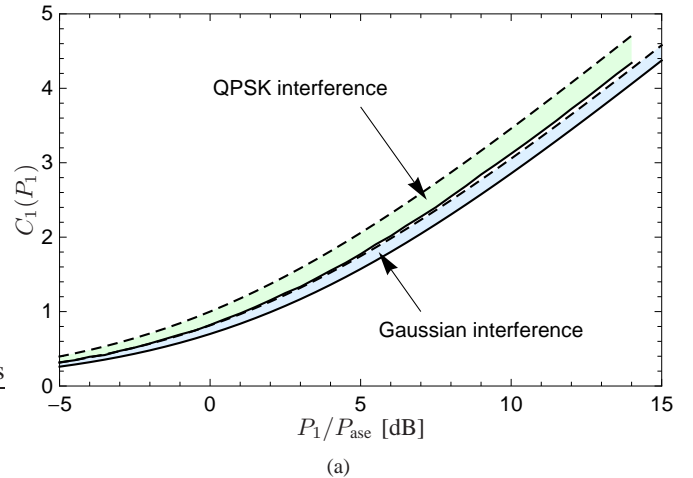


Fig. 2. The achievable rates $C_1(P_1)$ of user 1 in a WDM system, with the three behavioral models (a), (b), and (c), defined in Sec. III, as a function of the signal power P_1 . Dashed lines give upper bounds and solid lines lower bounds. Shaded regions indicate the amount of uncertainty. Behavioral models (a) and (b) both have two versions, depending on the type of interferer distributions. In (c), the lower bound is obtained as the envelope of multiple bounds, indicated with gray curves. Dotted vertical lines correspond to curves in Fig. 3.

discrete input distributions for the interfering channels than in the Gaussian case, but the capacity follows the same general trend in both cases.

B. Behavioral model (b)—adaptive interferer power

With behavioral model (b), the power of all users is the same, but the distributions may be different. The same upper and lower bounds as in Fig. 2 (a) are plotted in Fig. 2 (b): Theorems 2 and 5 with QPSK interference and Theorems 3 and 8 with Gaussian interference. With this behavioral model, the achievable rate of the primary channel is fundamentally different depending on the nature of the interference. If the interferers' distributions are discrete, the achievable rate increases with power towards infinity. This can be intuitively understood as follows. The magnitude of the interference term $\epsilon X_2^2 X_3^*$ will, at high enough power $P_1 = P_2 = P_3$, be much larger than X_1 or N_1 . Hence, receiver 1 can detect the value of $\epsilon X_2^2 X_3^*$ with high reliability (only four values are possible in the QPSK case) and subtract this value from the received signal Y_1 . After this so-called *interference cancellation*, subchannel 1 is effectively an AWGN channel $X_1 + N_1$, whose capacity is $\log_2(1 + P_1/P_{\text{ase}})$. This is the reason why the two bounds converge near $P_1/P_{\text{ase}} = 14$ dB and above. However, no similar receiver strategy is possible if X_2 and X_3 are Gaussian³, because then $\epsilon X_2^2 X_3^*$, which has a continuous distribution with large variance, effectively drowns the weaker contribution from X_1 . Therefore, this achievable rate has a peak at a moderate power, after which it decreases towards zero for very high power, as seen in Fig. 2 (b).

C. Behavioral model (c)—adaptive interferer distribution

To obtain a lower bound with behavioral model (c), i.e., when all users apply the same input distribution, we apply Theorem 4 with a suitably chosen input distribution $f_{X_1} = f_{X_2} = f_{X_3}$. For the same reasons as in Fig. 2 (b), a discrete input distribution is advantageous when the interference is strong. We therefore consider M -PSK constellations with uniform probabilities and choose the integer M suitably, as described in the following.

The bounds with behavioral model (c) are illustrated in Fig. 2 (c). The upper bound is again Theorem 2. The lower bound is obtained from Theorem 4 as discussed in the previous paragraph. Each $M = 2, \dots, 16$ gives rise to one lower bound, indicated in gray. As visible in the bottom right of the figure, each of these bound converge to $\log_2 M$ at high power. This can be understood as follows. As explained in Sec. VII-B, the interference term $\epsilon X_2^2 X_3^*$ in (1) can be reliably detected by receiver 1 and subtracted from Y_1 . This holds for any discrete constellation at sufficiently high power. After interference cancellation, the effective channel is again $X_1 + N_1$, whose mutual information with a uniform M -PSK input distribution is asymptotically $\log_2 M$. Hence, for every M , there exists a power threshold above which the lower bound is arbitrarily

³As stated in Sec. II, no receiver knows any of the other subchannels' codebooks. If these codebooks were known, the interference can be detected and subtracted even for Gaussian X_2 and X_3 . [2, Sec. 15.1.5].

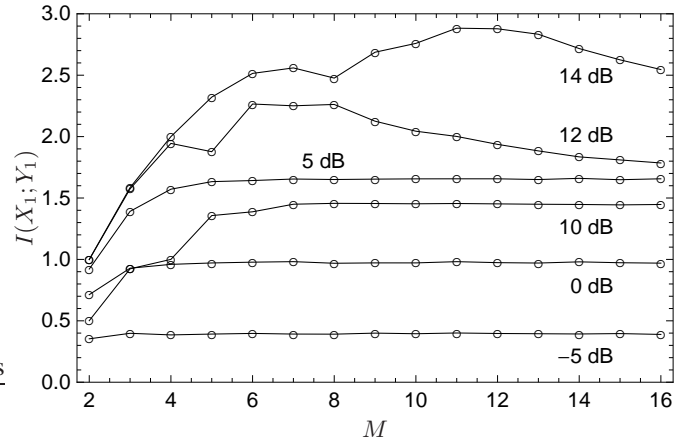


Fig. 3. The mutual information according to Theorem 4 for M -PSK constellations with uniform probabilities, for the indicated values of P_1/P_{ase} . The peak of each curve yields the lower bound in Fig. 2 (c).

close to $\log_2 M$. This proves that the envelope of these bounds, shown in black in Fig. 2 (c), grows unboundedly.

The optimization process is illustrated in Fig. 3, which shows the mutual information $I(X_1; Y_1)$ according to Theorem 4 as a function of $M = 2, \dots, 16$, for selected values of P_1/P_{ase} . At low signal power, the mutual information is practically the same for any M -PSK constellation (and actually for any zero-mean distribution, including Gaussian), whereas the optimal M tends to increase with power in the nonlinear regime. We know for sure that M -PSK are not optimal constellations⁴, but they suffice to show the qualitative trend of the achievable rate: It again grows with increasing power towards infinity. This result is significantly stronger than the theoretical prediction for this behavioral model with arbitrary channel models [12], which only states that the achievable rate is nondecreasing.

VIII. CONCLUSIONS AND DISCUSSION

Multuser information theory, or network information theory, is still in its infancy. In the information theory literature, the most common approach is to study the multuser capacity region, i.e., the set of achievable rates for all users simultaneously. In this work, however, we followed the most common approach in optical communications, which is to study the channel capacity of a single user in the system. More specifically, we considered the achievable rate of a single wavelength in a multuser WDM system, assuming certain behavioral models for the transmission on the other wavelengths.

For behavioral models (a) and (c), the achievable rate is unbounded with the signal power. With model (b), however, the outcome depends crucially on the distributions on the interfering channels; the achievable rate may increase indefinitely, as with the other behavioral models, or it may decrease to zero as the signal power increases. These results were obtained by analytically deriving both upper and lower bounds, in contrast

⁴E.g., a satellite constellation [11] would improve the lower bound, at least in the range between 6 and 11 dB.

to most previous works, which have studied lower bounds alone.

On a theoretical level, the most important conclusion in this paper is that the results depend strongly on the assumed behavioral model. We emphasize that whenever a single-channel model is derived for a multiuser system, there is always an underlying behavioral model involved. However, despite their significance, behavioral models have not yet received much attention in optical communications. Our recommendation to everyone working with the capacity of such single-user channel models is to clearly state and justify the behavioral model, because it has such a profound impact on the end results.

On a more practical level, the main message is that unbounded capacity growth is indeed possible, under some specific conditions: (i) The interferers use discrete constellations; (ii) the channel model depends on the actual signals transmitted by all users, not on the statistical properties of signals [13], [30]; (iii) the symbol clocks of different users are synchronized; and (iv) the receiver applies multiuser detection [27], [33], [34].

The results were computed for a dispersionless three-user WDM model (1)–(3), derived in the weakly nonlinear regime. Despite its simplicity, this channel model serves to illustrate the fundamental differences between behavioral models. Future work may involve extending the channel model to the strongly nonlinear regime or accounting for dispersion, more users (wavelength channels), or dual polarization. It is not known to which extent the conclusions above extend to such more realistic channels.

ACKNOWLEDGMENT

We wish to acknowledge inspiring discussions with colleagues within the Chalmers FORCE center.

REFERENCES

- [1] C. E. Shannon, "A mathematical theory of communication," *Bell System Technical Journal*, vol. 27, pp. 379–423, 623–656, July, Oct. 1948.
- [2] T. M. Cover and J. A. Thomas, *Elements of Information Theory*, 2nd ed. Hoboken, NJ: Wiley, 2006.
- [3] A. Splett, C. Kurtzke, and K. Petermann, "Ultimate transmission capacity of amplified optical fiber communication systems taking into account fiber nonlinearities," in *Proc. European Conference on Optical Communication (ECOC)*, Montreux, Switzerland, Sept. 1993, pp. 41–44.
- [4] P. P. Mitra and J. B. Stark, "Nonlinear limits to the information capacity of optical fibre communications," *Nature*, vol. 411, pp. 1027–1030, June 2001.
- [5] R.-J. Essiambre, G. Kramer, P. J. Winzer, G. J. Foschini, and B. Goebel, "Capacity limits of optical fiber networks," *J. Lightw. Technol.*, vol. 28, no. 4, pp. 662–701, Feb. 2010.
- [6] A. D. Ellis, J. Zhao, and D. Cotter, "Approaching the non-linear Shannon limit," *J. Lightw. Technol.*, vol. 28, no. 4, pp. 423–433, Feb. 2010.
- [7] A. Mecozzi and R.-J. Essiambre, "Nonlinear Shannon limit in pseudolinear coherent systems," *J. Lightw. Technol.*, vol. 30, no. 12, pp. 2011–2024, June 2012.
- [8] K. S. Turitsyn, S. A. Derevyanko, I. V. Yurkevich, and S. K. Turitsyn, "Information capacity of optical fiber channels with zero average dispersion," *Physical Review Letters*, vol. 91, no. 20, pp. 203 901–1–4, Nov. 2003.
- [9] R.-J. Essiambre, G. J. Foschini, G. Kramer, and P. J. Winzer, "Capacity limits of information transport in fiber-optic networks," *Physical Review Letters*, vol. 101, no. 16, pp. 163 901–1–4, Oct. 2008.
- [10] I. B. Djordjevic, "Codes on graphs, coded modulation and compensation of nonlinear impairments by turbo equalization," in *Impact of Nonlinearities on Fiber Optic Communications*, S. Kumar, Ed. New York, NY: Springer, 2011, ch. 12, pp. 451–505.
- [11] E. Agrell and M. Karlsson, "Satellite constellations: Towards the non-linear channel capacity," in *Proc. IEEE Photonics Conference (IPC)*, Burlingame, CA, Sept. 2012, pp. 316–317.
- [12] E. Agrell, "Conditions for a monotonic channel capacity," *IEEE Trans. Commun.*, vol. 63, no. 3, pp. 738–748, Mar. 2015.
- [13] E. Agrell, A. Alvarado, G. Durisi, and M. Karlsson, "Capacity of a nonlinear optical channel with finite memory," *J. Lightw. Technol.*, vol. 32, no. 16, pp. 2862–2876, Aug. 2014.
- [14] E. Agrell and M. Karlsson, "WDM channel capacity and its dependence on multichannel adaptation models," in *Proc. Optical Fiber Communication Conference (OFC)*, Anaheim, CA, Mar. 2013, p. OTu3B.4.
- [15] J. B. Stark, P. Mitra, and A. Sengupta, "Information capacity of nonlinear wavelength division multiplexing fiber optic transmission line," *Optical Fiber Technology*, vol. 7, no. 4, pp. 275–288, Oct. 2001.
- [16] J. Tang, "The channel capacity of multispan DWDM system employing dispersive nonlinear optical fibers and an ideal coherent optical receiver," *J. Lightw. Technol.*, vol. 20, no. 7, pp. 1095–1101, Apr. 2002.
- [17] K.-P. Ho and J. M. Kahn, "Channel capacity of WDM systems using constant-intensity modulation formats," in *Proc. Optical Fiber Communication Conference (OFC)*, Anaheim, CA, Mar. 2002, pp. 731–733.
- [18] A. G. Green, P. B. Littlewood, P. P. Mitra, and L. G. L. Wegener, "Schrödinger equation with a spatially and temporally random potential: Effects of cross-phase modulation in optical communication," *Physical Review E*, vol. 66, no. 4, pp. 046 627–1–12, Oct. 2002.
- [19] J. M. Kahn and K.-P. Ho, "Spectral efficiency limits and modulation/detection techniques for DWDM systems," *IEEE Journal of Selected Topics in Quantum Electronics*, vol. 10, no. 2, pp. 259–272, Mar./Apr. 2004.
- [20] L. G. L. Wegener, M. L. Povinelli, A. G. Green, P. P. Mitra, J. B. Stark, and P. B. Littlewood, "The effect of propagation nonlinearities on the information capacity of WDM optical fiber systems: cross-phase modulation and four-wave mixing," *Physica D: Nonlinear Phenomena*, vol. 189, no. 1–2, pp. 81–99, Feb. 2004.
- [21] J. Tang, "A comparison study of the Shannon channel capacity of various nonlinear optical fibers," *J. Lightw. Technol.*, vol. 24, no. 5, pp. 2070–2075, May 2006.
- [22] T. Freckmann, R.-J. Essiambre, P. J. Winzer, G. J. Foschini, and G. Kramer, "Fiber capacity limits with optimized ring constellations," *IEEE Photon. Technol. Lett.*, vol. 21, no. 20, pp. 1496–1498, Oct. 2009.
- [23] A. D. Ellis and J. Zhao, "Channel capacity of non-linear transmission systems," in *Impact of Nonlinearities on Fiber Optic Communications*, S. Kumar, Ed. New York, NY: Springer, 2011, ch. 13, pp. 507–538.
- [24] G. Bosco, P. Poggiolini, A. Carena, V. Curri, and F. Forghieri, "Analytical results on channel capacity in uncompensated optical links with coherent detection," *Opt. Exp.*, vol. 19, no. 26, pp. B440–B449, Dec. 2011.
- [25] R.-J. Essiambre and A. Mecozzi, "Capacity limits in single-mode fiber and scaling for spatial multiplexing," in *Proc. Optical Fiber Communication Conference (OFC)*, Los Angeles, CA, Mar. 2012, p. OW3D.1.
- [26] M. Secondini, E. Forestieri, and G. Prati, "Achievable information rate in nonlinear WDM fiber-optic systems with arbitrary modulation formats and dispersion maps," *J. Lightw. Technol.*, vol. 31, no. 23, pp. 3839–3852, Dec. 2013.
- [27] M. H. Taghavi, G. C. Papen, and P. H. Siegel, "On the multiuser capacity of WDM in a nonlinear optical fiber: coherent communication," *IEEE Trans. Inf. Theory*, vol. 52, no. 11, pp. 5008–5022, Nov. 2006.
- [28] A. El Gamal and Y.-H. Kim, *Network Information Theory*. Cambridge, UK: Cambridge University Press, 2011.
- [29] G. Cappellini and S. Trillo, "Third-order three-wave mixing in single-mode fibers: Exact solutions and spatial instability effects," *Journal of the Optical Society of America B*, vol. 8, no. 4, pp. 824–838, Apr. 1991.
- [30] E. Agrell, G. Durisi, and P. Johannisson, "Information-theory-friendly models for fiber-optic channels: A primer," in *Proc. IEEE Information Theory Workshop (ITW)*, Jerusalem, Israel, Apr.–May 2015.
- [31] M. Eiselt, "Limits on WDM systems due to four-wave mixing: A statistical approach," *J. Lightw. Technol.*, vol. 17, no. 11, pp. 2261–2267, Nov. 1999.
- [32] F. Forghieri, R. W. Tkach, and A. R. Chraplyvy, "Fiber nonlinearities and their impact on transmission systems," in *Optical Fiber Telecommunications IIIA*, I. P. Kaminov and T. L. Koch, Eds. San Diego, CA: Academic Press, 1997, ch. 8, pp. 196–255.
- [33] B. Xu and M. Brandt-Pearce, "Multiuser detection for square-law receiver under Gaussian channel noise with applications to fiber-optic communications," *IEEE Trans. Inf. Theory*, vol. 51, no. 7, pp. 2657–2664, July 2005.

- [34] —, “Multiuser square-law detection with applications to fiber optic communications,” *IEEE Trans. Commun.*, vol. 54, no. 7, pp. 1289–1298, July 2006.
- [35] D. M. Arnold, H.-A. Loeliger, P. O. Vontobel, A. Kavčić, and W. Zeng, “Simulation-based computation of information rates for channels with memory,” *IEEE Trans. Inf. Theory*, vol. 52, no. 8, pp. 3498–3508, Aug. 2006.
- [36] F. M. Reza, *An Introduction to Information Theory*. New York, NY: McGraw-Hill, 1961.
- [37] A. Papoulis, *Probability, Random Variables, and Stochastic Processes*, 3rd ed. New York, NY: McGraw-Hill, 1991.